Available online at www.sciencedirect.com

SCIENCE DIRECT®

Earth and Planetary Science Letters 232 (2005) 179–191

EPSL

www.elsevier.com/locate/epsl

Numerical ages for Plio-Pleistocene glacial sediment sequences by $^{26}Al/^{10}Be$ dating of quartz in buried paleosols

Greg Balco[a,*], John O.H. Stone[a], Joseph A. Mason[b]

[a]*Quaternary Research Center and Department of Earth and Space Sciences, University of Washington, Mail Stop 351310, Seattle, WA 98195-1310, USA*

[b]*Department of Geography, University of Wisconsin, 550 North Park Street, Madison, WI 53706, USA*

Received 12 March 2004; received in revised form 16 November 2004; accepted 15 December 2004

Editor: K. Farley

Abstract

We describe a method for dating Plio-Pleistocene sediments by analysing ^{26}Al and ^{10}Be in quartz from buried paleosols. The method amounts to a generalization of the technique of "burial dating," which has previously been used to date river sands deposited in caves as well as fluvial terraces. We (a) measure nuclide concentrations at multiple depths in the paleosol; (b) use the geologic context of the sample to construct an exposure/burial history (an "exposure model") that can be used to predict the nuclide concentrations in the samples as a function of whatever unknown parameters are of geological interest (e.g., the ages of geologic units); and then (c) find the parameters in the exposure model that result in the best fit between predicted and observed nuclide concentrations. We apply the method to a paleosol developed on the uppermost till in eastern Nebraska, which is buried by several middle to late Pleistocene loess units, the ages of some of which are known independently. The lowest loess unit, whose age was not previously known, was deposited 0.58 ± 0.12 Ma, and the till was emplaced 0.65 ± 0.14 Ma, which agrees with existing age constraints from paleomagnetic measurements and the position of the Lava Creek ash in the regional stratigraphy. The most important source of uncertainty in these age determinations is the analytical uncertainty in ^{26}Al and ^{10}Be measurements; uncertainties in either the nuclide production rates or the geologic model are comparatively unimportant.

Keywords: cosmogenic nuclides; Beryllium-10; Aluminum-26; Quaternary geochronology; paleosols; Nebraska; Pleistocene

1. Introduction

In this paper we describe a means of dating Plio-Pleistocene sediments using the cosmic-ray-produced radionuclides ^{26}Al and ^{10}Be. We are motivated by the need for better dating of terrestrial glacial deposits that

* Corresponding author. Tel.: +1 206 221 6383.
E-mail addresses: balcs@u.washington.edu (G. Balco), stone@geology.washington.edu (J.O.H. Stone), mason@geography.wisc.edu (J.A. Mason).

0012-821X/$ - see front matter © 2005 Elsevier B.V. All rights reserved.
doi:10.1016/j.epsl.2004.12.013

predate the last two glaciations. Thick, well-exposed, and well-studied sequences of tills and related glacial and interglacial sediments are widely distributed in North America and Eurasia, but most information about the timing of pre-late Pleistocene glaciations actually comes from oxygen-isotope records in marine sediment cores [1,2]. Such marine $\delta^{18}O$ time series record only global ice volume: except in rare cases where ice-rafted debris can be associated with a particular source [3–5], they give no information about the location of ice sheets on the continents or the distribution of ice between different ice sheets. The continental deposits that would provide this information are extremely difficult to date. For example, the only existing means of dating past advances of the Laurentide Ice Sheet that are older than the useful ranges of radiocarbon (~50,000 yr) or optical dating techniques (~150,000 yr) is to bracket their deposits between two easily recognized magnetic reversals at 0.78 and 2.58 Ma [6], or three widespread volcanic ashes from the Yellowstone volcanic center at 0.6, 1.3, and 2.0 Ma [7]. As only a few sections contain any of these time markers at all, it is impossible to associate most pre-Wisconsinan tills with particular marine oxygen isotope stages.

In an effort to better date terrestrial glacial sediments and improve correlation of marine paleoclimate records with terrestrial glacial records, therefore, we are applying cosmogenic-nuclide techniques to determine the age of glacial sediment sequences. In this paper we describe such a method for dating sediments that overlie buried paleosols, which are common in Plio-Pleistocene glacial sequences surrounding the Laurentide and other ice sheets. Although we are concerned here with glacial sediments, we aim to provide a general method that can be adapted to many other depositional settings.

2. Basic idea of the method

^{26}Al and ^{10}Be are rare radionuclides that are produced at a fixed ratio in quartz grains subjected to cosmic ray bombardment at the Earth's surface, but have different decay constants. They are commonly used in exposure-dating studies [8]. If quartz exposed at the Earth's surface for enough time to accumulate a significant concentration of these nuclides is then deeply buried–and thus isolated from the cosmic-ray flux–the two nuclides decay at different rates, and the $^{26}Al/^{10}Be$ ratio reflects the duration of burial. This idea is the basis of the "burial dating" method described by Klein et al. [9] and Granger and Muzikar [10], which has been used primarily to date river sediment carried into caves and abandoned [11]. In this form, "burial dating" consists of assuming that the sediment sample began with zero initial ^{26}Al and ^{10}Be concentrations, accumulated ^{26}Al and ^{10}Be as it was brought to the surface by steady erosion of a landscape continuously exposed to cosmic rays, and then was rapidly transported and buried at a depth sufficient to greatly reduce the cosmic ray flux. This exposure/burial history has two unknown parameters: the erosion rate at the sediment source, and the duration of burial. As there are also two measurements–the observed ^{26}Al and ^{10}Be concentrations–the unknown parameters are single-valued functions of the measurements. Granger and Muzikar [10] provide formulae for determining the burial age in this situation.

The example of river sediment in caves is a specific case of a more general approach, which consists of: (a) using the geologic context of the sample to construct an exposure/burial history (which we refer to as an "exposure model"); (b) including in the exposure model whatever unknown parameters are of geological interest (e.g., the ages of certain units); and (c) finding the parameters in the exposure model that best predict the observed nuclide concentrations in the sample. In the case of cave sediment, the exposure model is that the sample has experienced one period of steady erosion and one of burial at constant depth, and the unknown parameters are the erosion rate before burial and the duration of burial. This basic idea, that of using geologic information to develop an exposure model, and then using ^{26}Al and ^{10}Be measurements to quantify the durations or the rates of the different events in the exposure model, can in principle be applied in a much wider variety of situations. In this paper we apply it to sequences of stratified sediments, where the exposure model is more complicated, there are more unknown parameters, and the mathematical approach is somewhat different. To summarize, the exposure model, i.e., the sequence of events whose ages or rates we hope to quantify, stems from the geomorphic and stratigraphic context of the sample, not from the ^{26}Al and ^{10}Be

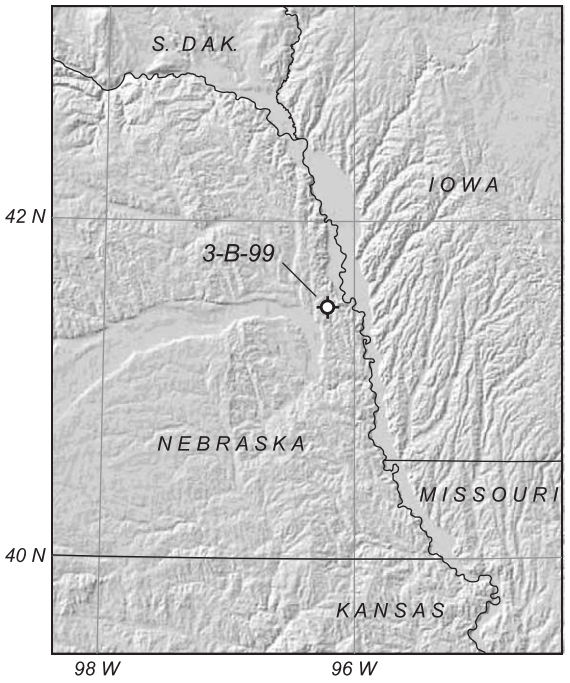

Fig. 1. Location of borehole 3-B-99.

measurements. We use geologic information to answer the question "what happened," and then use cosmogenic-nuclide measurements to answer the questions "when," or "how fast." In some cases, the ^{26}Al and ^{10}Be measurements may help to choose between two possible sequences of events that cannot be distinguished by geologic evidence alone (we give an example of this later on), but, in general, correctly interpreting the geologic history of the samples is more important than the precision of the ^{26}Al and ^{10}Be measurements, or the accuracy of nuclide production rates, in obtaining accurate ages.

In the example we discuss in this paper, we collected samples from a paleosol developed on the surface of a middle Pleistocene till, which has been buried by one loess unit of unknown age and two additional loess units of independently known age. Thus, the exposure model consists of the initial emplacement of the till, a period of surface exposure and slow erosion during which the soil formed, and three periods of burial under successively increasing thicknesses of overburden. The unknown parameters consist of the initial ^{26}Al and ^{10}Be concentrations in the till at the time of emplacement, the age of the till, the duration of soil formation, the erosion rate during soil formation, and the age of the lowermost loess unit. Although this situation is similar to the "burial dating" approach used for cave sediments in that the samples have been exposed near the surface for a time and then buried for a time, it violates three of the key assumptions of that method: the initial nuclide concentrations in the till are likely not zero, the surface was probably not exposed long enough to reach equilibrium with a steady erosion rate, and the burial depth changed repeatedly. If we were to ignore these complications, we would expect to obtain incorrect ages. In order to do better, we need a more complicated exposure model which incorporates both the known and unknown aspects of the depositional history, a larger number of data to constrain the unknowns, and a different mathematical framework. We describe all these elements below.

3. Example: glacial sediments in borehole 3-B-99, eastern Nebraska

Nebraska Conservation and Survey Division borehole 3-B-99 penetrates four loess units which are separated by paleosols and which overlie another paleosol developed in till (Figs. 1 and 2; [12]). This till most likely correlates with a till in nearby sections that is normally magnetized and underlies the 0.6 Ma Lava Creek ash [13,14]. Table 1 describes the paleosol which forms the top of this till. This paleosol is

Table 1
Soil description

Borehole depth (m)	Description
26.00–26.21	Ab. 10YR 4/3 clay, strong fine subangular blocky structure.
26.21–26.58	Bt1b. 10YR 5/3 clay (5% gravel), strong fine subangular blocky structure, clay coatings on ped faces.
26.58–27.11	Bt2b. 7.5YR 4/4 clay (5% gravel), moderate fine subangular blocky parting to moderate very fine subangular blocky structure.
27.11–27.40	BCb. 10YR 5/6 clay (5% gravel), moderate fine subangular blocky structure, clay coatings on ped faces.
27.40–28.65+	C. 2.5Y 5/6 clay (10% gravel), moderate medium subangular blocky structure, effervescent in 10% HCl.

overlain by 8.5 m of clay-rich, pedogenically altered loess of unknown age (the 'silty clays' of [12]), then by 7.6 m of Loveland loess (deposited ca. 135,000–150,000 yr B.P.), and finally by 10.3 m of Gilman Canyon Formation and Peoria Loess (deposited 35,000–12,000 yr B.P) [12,15–17]. Thus, the sequence of events represented here consists of the initial emplacement of the till, a period of non-deposition and soil formation, and three (we group the Gilman Canyon and Peoria loesses together because they are close in age) episodes of loess deposition separated by periods of stability and soil formation. We are interested in determining the ages of the lowest loess unit and the till.

4. Analytical methods

We measured ^{26}Al and ^{10}Be concentrations in quartz extracted from core samples of pedogenically altered till from the prominent paleosol between 26.0 and 28.1 m depth. We disaggregated core samples by soaking in water and $(NaPO_3)_6$ ("Calgon") in an ultrasonic bath, then isolated the 0.125–0.85 mm grain size by wet-sieving. We extracted and purified quartz by repeated etching in 2% HF, heavy-liquid separation to remove refractory heavy minerals, soaking in hot KOH to remove secondary fluoride precipitated during the HF treatment, and a final 2% HF etch. This procedure yielded quartz with 60–80 ppm total Al. We extracted Al and Be from quartz using standard methods [18,19], prepared Al cathodes by Al–Ag coprecipitation [20], and measured isotope ratios at the Lawrence Livermore National Laboratory, Center for Accelerator Mass Spectrometry. Combined process and carrier blanks were $6.3\pm6.5\times10^4$ atoms ^{26}Al and $2.6\pm0.3\times10^5$ atoms ^{10}Be. Table 2 shows the results.

In order to calculate nuclide production rates, we need to know the shielding depth of samples below the surface in g cm^{-2}. To determine this, we measured the density of our samples by an adaptation of the procedure outlined in [21] (also see [22]). We used the dry density determined by this method (1.92 ± 0.08 g cm^{-3}) to calculate shielding depths during soil formation. We based our calculation of shielding depths during burial by loess units on previous measurements of loess density in eastern Nebraska (J. Mason, unpublished data). We assumed that, at any time, the upper 15 m of loess was not water-saturated and had a bulk density of 1.9 g cm^{-3}; underlying loess was water-saturated, with a bulk density of 2.3 g cm^{-3}. We discuss the effect of uncertainties in this assumption later.

5. Mathematical description of the exposure model

Our goal in this section is to create a function whose arguments are the unknown parameters of interest (in particular, the ages of geologic units), that predicts the ^{26}Al and ^{10}Be concentrations in our samples, and computes how well these predictions match the measured concentrations. Once armed with this function, we can look for the parameter values that result in the best fit between the predicted and measured nuclide concentrations.

We can predict ^{26}Al and ^{10}Be concentrations in a sample for any arbitrary exposure history by solving

Table 2
^{10}Be and ^{26}Al analyses

Sample ID	Borehole depth (m)	Depth below soil surface (g cm^{-2})	Effective depth[a] (g cm^{-2})	^{10}Be[b] (10^4 atoms g^{-1})	^{26}Al[b] (10^4 atoms g^{-1})
3-B-99-87	26.01–26.31	0–58	28	31.88±1.08	133.8±4.3
3-B-99-88	26.31–26.62	58–117	87	26.83±0.93	112.7±3.3
3-B-99-89	26.62–26.92	117–175	145	19.75±0.58	85.6±3.8
3-B-99-90	27.07–27.23	204–234	219	16.14±0.49	67.6±3.5
3-B-99-91	27.32–27.46	234–278	256	15.75±0.47	57.9±2.1
3-B-99-93[c]	27.76–28.14	336–410	372	11.92±0.28	48.7±1.9

[a] The effective depth is the depth at which the production rate is the same as the mean production rate in the entire sample interval.
[b] Measured relative to LLNL internal standards. Uncertainties are shown at $\pm1\sigma$ and include all known sources of analytical error.
[c] Mean of two analyses.

the differential equation governing nuclide production and decay:

$$\frac{dN_{i,j}}{dt} = P_j(z_i(t)) - N_{i,j}\lambda_j \quad (1)$$

where the subscript i indicates the sample number: i=1…6, and the subscript j indicates the nuclide measured, i.e., j=10 for ^{10}Be and j=26 for ^{26}Al. $N_{i,j}$ is the concentration (atoms g^{-1}) of nuclide j in sample i, $P_j(z)$ is the production rate (atoms g^{-1} yr^{-1}) of nuclide j at depth z, and λ_j is the decay constant (yr^{-1}) for nuclide j. The important part of this equation is the age/depth function $z_i(t)$, where z_i is the depth (g cm^{-2}) of sample i below the surface. We derive $z_i(t)$ from the geologic history: the paleosol experienced one period of surface exposure followed by three periods of steadily deeper burial, so $z(t)$ is a step function as shown in Fig. 2.

There are three important assumptions encapsulated in our choice of the age/depth function $z(t)$. First, we assume that all depositional events are recorded in the stratigraphy; that is, no additional units were deposited and then later removed without leaving any evidence. We justify this by the observation that the stratigraphy in this borehole closely duplicates that of many other boreholes in eastern Nebraska [12], none of which contain any additional units: thus, it is unlikely that there were any unrecorded episodes of deposition. Furthermore, the thickness of all the loess units is consistent among these boreholes (gradually thickening from west to east across the region), which suggests that the present thicknesses of the loess units in our borehole are close to the original depositional thicknesses, and were not affected by localized erosion. Second, we assume that each loess unit was deposited rapidly, which in this context means over 10^3 to 10^4, rather than 10^5, years. The upper loess units are in fact massive and display pedogenic alteration only near their tops, which indicates rapid deposition followed by soil formation. The lowest loess, on the other hand, is enriched in clay, and multiple soil profiles are present at some sites, suggesting that it may have accumulated gradually over a relatively long period of time. Here the geologic evidence is inconclusive with respect to the choice of $z(t)$; we show later that the ^{26}Al and ^{10}Be measurements are more consistent with rapid accumulation of the lowest loess than with gradual accumulation. Third, we assume that there was no erosion during the initial period of soil formation after till emplacement, which is unlikely to be true. This simplification arises because, although we could

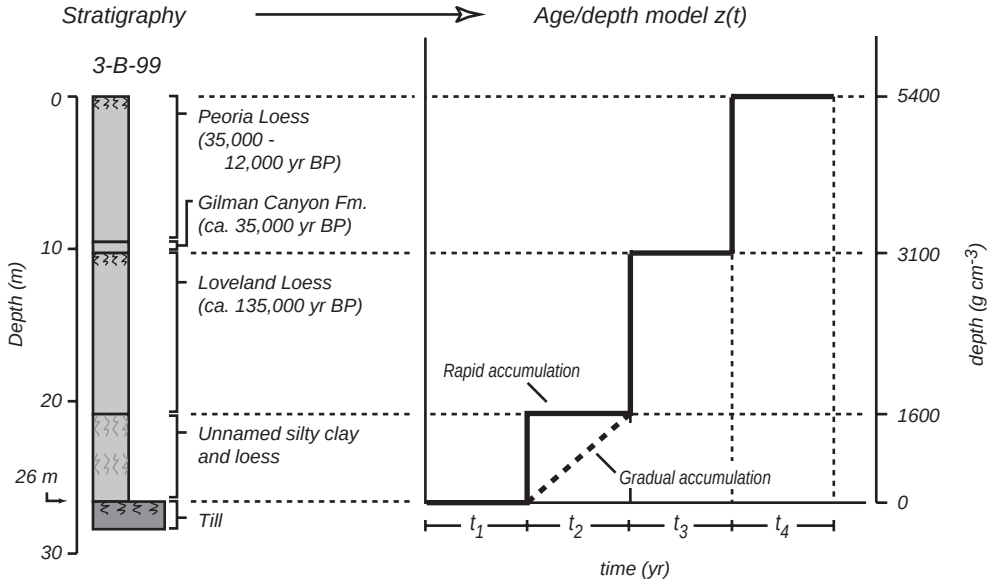

Fig. 2. Stratigraphy of borehole 3-B-99 ([12]) and resulting age/depth model for the surface of the paleosol at 26 m. The solid line denotes the age model in which the lowest loess accumulates rapidly; the dotted line shows the alternative age model in which it accumulates gradually.

account for surface erosion as well as exposure time when predicting the nuclide concentrations at the end of the period of soil formation, these two parameters have similar effects which cannot be distinguished without unusually precise ^{26}Al and ^{10}Be measurements. This difficulty is well known in exposure dating, and [23] discuss it in detail. In principle we could circumvent this difficulty by collecting samples from several meters below the soil surface (e.g., [24,25]), but we were unable to do so here because we reached the end of the drillcore. The eventual result of this simplification, where we retain the duration of exposure and soil formation as an unknown parameter in the exposure model, but disregard the surface erosion rate during this time period, is that we must make assumptions about the soil erosion rate in order to calculate the age of the till. We discuss this in more detail later.

We could numerically integrate Eq. (1) to determine the expected nuclide concentrations at the end of any arbitrarily complicated exposure history. However, as we have chosen a step function for $z(t)$, we can use a simple analytical solution. We denote the successive periods of exposure or burial at different depths by the subscript k, where k=1…K. In this example, K=4. At the end of time period k, the concentration of nuclide j in sample i is $N_{i,j,k}$, such that:

$$N_{i,j,k} = N_{i,j,(k-1)} e^{-\lambda_j t_k} + \frac{P_j(z_{i,k})}{\lambda_j}\left(1 - e^{-\lambda_j t_k}\right) \qquad (2)$$

where t_k is the duration of time period k (yr) and $z_{i,k}$ is the depth (g cm^{-2}) of sample i during time period k. The two parts of this equation include, first, decay of the nuclide concentration that was present at the beginning of the time period, and, second, new nuclide production during the time period.

We know most of the parameters needed to evaluate this equation. First, the depths $z_{i,k}$ reflect the measured stratigraphy in the borehole. The depths $z_{i,1}$ during the first period of exposure and soil formation are simply the measured depths of the samples below the soil surface. As the samples consist of 0.3-m sections of drill-core, we integrated $P(z)$ over the depth range of each sample to derive an value for $z_{i,1}$ such that the production rate at that depth is equal to the average production rate over the entire sample thickness. Table 2 shows these values. We computed $z_{i,2}…z_{i,4}$ simply by adding the thickness of the successive layers of overburden (Fig. 2) to the values of $z_{i,1}$.

To derive the production rates $P_j(z_{i,k})$, we calculate the surface production rates according to [26], assume that production by muons follows the approximation for sea level and high latitude given in [27] and [28], apportion the remainder of surface production to spallation reactions, and assume that production by spallation reactions decreases exponentially with depth with an attenuation length of 160 g cm^{-2}. The surface production rates at this site are 6.9 and 42.1 atoms g^{-1} yr^{-1} for ^{10}Be and ^{26}Al, respectively. The use of a sea level/high latitude compilation of muon flux measurements results in inaccurate production rates at moderate depths (ca. 500–2000 g cm^{-2}); however, as we discuss later this uncertainty does not significantly affect our results.

There are two important hidden assumptions in assigning production rates during the first time period of exposure and soil formation in this way. First, we assume that the true soil surface is preserved in the section. In this example, the presence of an Ab horizon indicates that the entire soil profile is in fact present. If we were applying this technique in a situation where the soil profile had been truncated during deposition of the overlying material, we would either have to infer the amount of truncation from the soil characteristics, or treat it as an additional unknown parameter. This would eventually result in additional uncertainty in determining the exposure time of the soil, but would not affect our ability to determine its burial age; thus, the lack of a complete soil profile is not necessarily an obstacle to using this technique to date overlying deposits. Second, we have assumed that the coarse-grained fraction of the soil which we have sampled was not mixed vertically. Illuvial clay coatings in the Bt horizons of the paleosol, as well as the presence of atmospherically produced ^{10}Be 1 m below the soil surface [29], do indicate vertical transport of fine particles. However, the measured ^{10}Be and ^{26}Al concentrations in the soil are indistinguishable from an exponential profile with an attenuation length of 160 g cm^{-2} (Fig. 3). If mixing of coarse sand between samples had been significant, this could not be the case. Although bioturbation and rooting must have taken place during soil formation, it

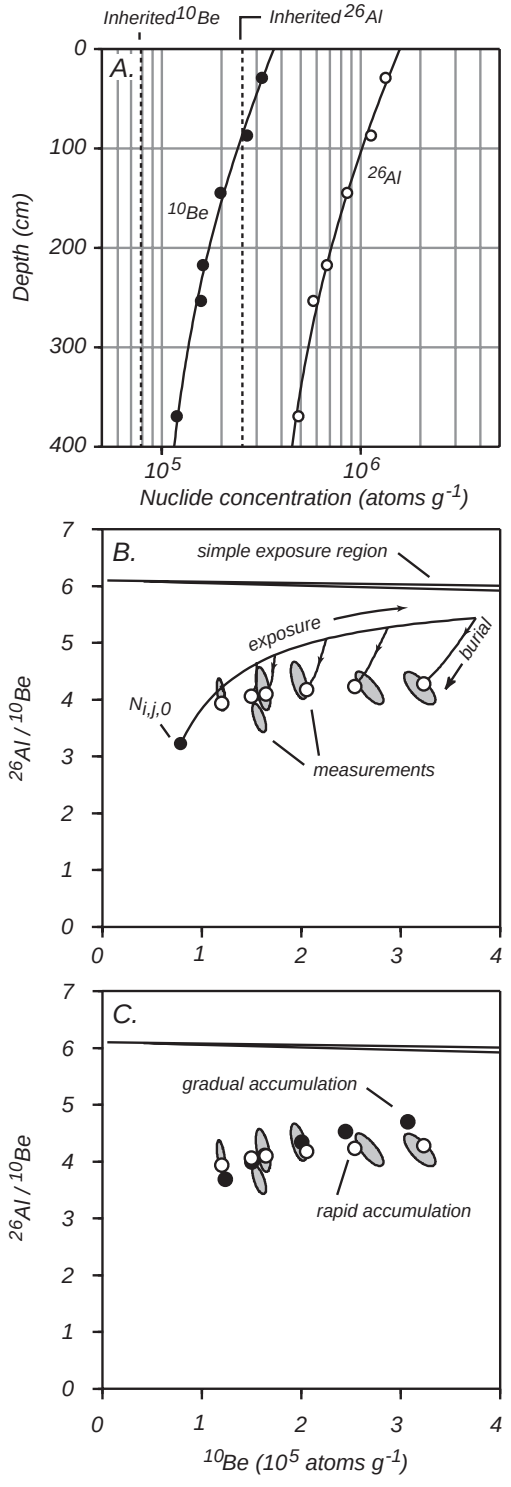

was apparently confined to the uppermost 30 cm, the thickness of our shallowest sample.

The decay constants are $\lambda_{10}=4.59\times10^{-7}$ yr^{-1} and $\lambda_{26}=9.78\times10^{-7}$ yr^{-1}. At present the correct value of λ_{10} is the subject of active research and some other authors use a different value of 5.18×10^{-7} yr^{-1} [11]; pending resolution of this ambiguity we have chosen the most commonly accepted value.

We know the parameters t_3 and t_4 from independent ages of the uppermost loess units: t_3=115,000 yr and t_4=35,000 yr. This leaves only four unknown parameters. First, the durations of the first two time periods t_1 and t_2 are unknown. Second, we cannot evaluate Eq. (2) for the first time period without initial nuclide concentrations $N_{i,j,0}$. As the parent material of the paleosol is a till which was likely derived from recycled surficial sediment that may itself have had a complex exposure history, we cannot assume that the nuclide concentrations in the till were zero at the time it was emplaced. However, as many geochemical measurements show that massive till is well-mixed at the outcrop scale, we can assume that the initial nuclide concentrations are the same for all samples i, i.e., $N_{1,j,0}=N_{2,j,0}=\ldots=N_{6,j,0}$, and we can describe these initial concentrations by two unknown parameters $N_{i,10,0}$ and $N_{i,26,0}$.

To summarize, we can predict the nuclide concentrations in our samples at the present time by starting with some initial nuclide concentrations in the till $N_{i,j,0}$, assigning values to the additional unknown

Fig. 3. (A) Measured ^{26}Al and ^{10}Be concentrations in quartz from the paleosol (circles) compared with the concentration profile predicted by the best-fit exposure model and parameters described in the text (solid lines). The standard errors of the measurements are smaller than the data points at this scale. The dotted lines indicate the inherited nuclide concentrations $N_{i,j,0}$ derived from the age calculation. (B) Graphical representation of the best-fit exposure model on the ^{26}Al–^{10}Be parametric diagram of [33] and [9]. The grey ellipses are 68% uncertainty regions for the measured nuclide concentrations; the white circles are the nuclide concentrations predicted by the best-fit exposure model; the dark circle shows the initial nuclide concentrations in the till at the time of emplacement inferred from the calculation; and the solid lines show the evolution of nuclide concentrations in the samples during soil formation and subsequent burial. (C) Comparison between nuclide concentrations predicted by best-fit exposure model that assumes rapid emplacement of the lowest loess (white circles), and those predicted by the best-fit exposure model that assumes gradual emplacement of this unit (black circles; see Fig. 2). The grey ellipses are 68% uncertainty regions for the measured nuclide concentrations.

parameters t_1 and t_2, and applying Eq. (2) repeatedly to arrive at the final nuclide concentrations $N_{i,j,K}$. We can then evaluate how well the predicted nuclide concentrations fit the measured ones. We denote the measured concentrations by $N_{i,j}^M$, and we use the χ^2 statistic to describe the misfit M between measured and simulated nuclide concentrations:

$$M = \sum_i \sum_j \left(\frac{N_{i,j,K} - N_{i,j}^M}{\sigma N_{i,j}^M} \right)^2 \quad (3)$$

where the values $\sigma N_{i,j}^M$ are the standard errors of the ^{10}Be and ^{26}Al measurements. Thus, M is a function of the four unknown parameters $N_{i,10,0}$, $N_{i,26,0}$, t_1, and t_2, and we can now seek the values of these parameters that minimize M and thus best fit the measurements.

5.1. Optimization method: constraints

We used standard methods in the MATLAB Optimization Toolbox [30] to find the values of the unknown parameters that minimize the misfit function M. There are several constraints on the allowed values of these parameters. First, all must be positive. Second, the $N_{i,j,0}$ must be within the so-called permissible region [9]. This means not only that $N_{i,j,0}<P_j(0)/\lambda_j$, where $P_j(0)/\lambda_j$ is the surface steady-state concentration, but also that initial nuclide concentrations must lie within or below the simple exposure region on Fig. 3, i.e.,

$$\left[\frac{-1}{\lambda_{26}} \ln\left(1 - \frac{N_{26}\lambda_{26}}{P_{26}(0)} \right) \right] \leq \left[\frac{-1}{\lambda_{10}} \ln\left(1 - \frac{N_{10}\lambda_{10}}{P_{10}(0)} \right) \right] \quad (4)$$

where $P_j(0)$ is the surface production rate of nuclide j. This latter constraint is nonlinear and undefined for some parameter values, which presents potential difficulties for the optimization algorithm. Furthermore, if the samples had been exposed in the past at a significantly different elevation, it would not be appropriate to use the value of $P_j(0)$ for the present sample location in this constraint. We can avoid these difficulties in this particular example because we expect the values $N_{i,j,0}$ to be relatively small, such that $N_{i,j,0}<<P_j(0)/\lambda_j$, in which case this constraint reduces to $N_{26,0}/N_{10,0}<6.1$.

The only numerical difficulty with minimizing the function M arises from the asymptotic behaviour of Eq. (2): the partial derivatives of M with respect to the time parameters t_k are very small when the t_k are large. This is easily addressed by using an appropriate initial guess.

6. Results

Using the stepped age/depth function that we describe above, the parameters that best fit the measured nuclide concentrations are: $N_{i,10,0}=7.8\times10^4$ atoms g^{-1}; $N_{i,26,0}=2.6\times10^5$ atoms g^{-1}; $t_1=52{,}000$ yr; and $t_2=421{,}500$ yr. Fig. 3B shows this best-fit exposure history graphically. The age of the lowest loess unit, therefore, is $t_2+t_3+t_4=571{,}000$ yr. The age of the till is nominally $t_1+t_2+t_3+t_4$, but, as we discuss above, this involves the assumption that there was no surface erosion during the period of soil formation. Thus, the age that we infer for the till depends on our assumptions about the erosion rate of the soil. Existing measurements of Pleistocene surface erosion rates in the midcontinental U.S. [31,32] are 3–8 μm yr^{-1}; with these erosion rates the age of the till is 625,000–690,000 yr. The initial nuclide concentrations $N_{i,j,0}$ are significantly greater than zero, and the initial ^{26}Al/^{10}Be ratio is significantly less than the production ratio. This indicates that the till did in fact contain quartz that had already experienced a complicated history of exposure and burial [29], and shows that if we had attempted to interpret the data without accounting for inherited nuclide concentrations, we would have obtained incorrect ages.

As we discuss above, the geologic evidence is uncertain as to whether the lowermost loess unit was deposited quickly or gradually. In order to explore this, we carried out the same optimization procedure with a different age/depth function in which the lowermost loess was gradually deposited over the time period t_2 (Fig. 2). We could not use Eq. (2) for this more complicated age/depth function, so we integrated Eq. (1) numerically. The best-fit burial history with this new age/depth function is very different from that for the step function in that we infer a much younger age of 290,000 yr for the lowermost loess and a corresponding age near 320,000 yr for the till. However, we reject these results for two reasons. First, the predicted nuclide concentrations for this burial history are a poor fit to

the measurements relative to the predicted nuclide concentrations for the step-function burial history (Fig. 3). Second, the presence of the 0.6 Ma Lava Creek ash above a correlative till in nearby sections indicates that this till is older than the ash. Thus, the data are not consistent with an age/depth history in which the lowest loess accumulated slowly, and we conclude that the unit did in fact accumulate rapidly. In this context, given the uncertainty in our measurements, 'rapidly' could allow for accumulation over several tens of thousands of years, which could allow for the soil development in this unit.

7. Error analysis

Besides the possibility that our model for the emplacement of the lowest loess unit is incorrect, which we will not consider further, there are three primary sources of uncertainty in the four parameters that we have estimated. First, the ^{26}Al and ^{10}Be measurements include analytical uncertainty. Second, the nuclide production rates are uncertain: the independently calibrated production rates that we used have inherent uncertainties, and our assumption that the original soil surface was preserved might have

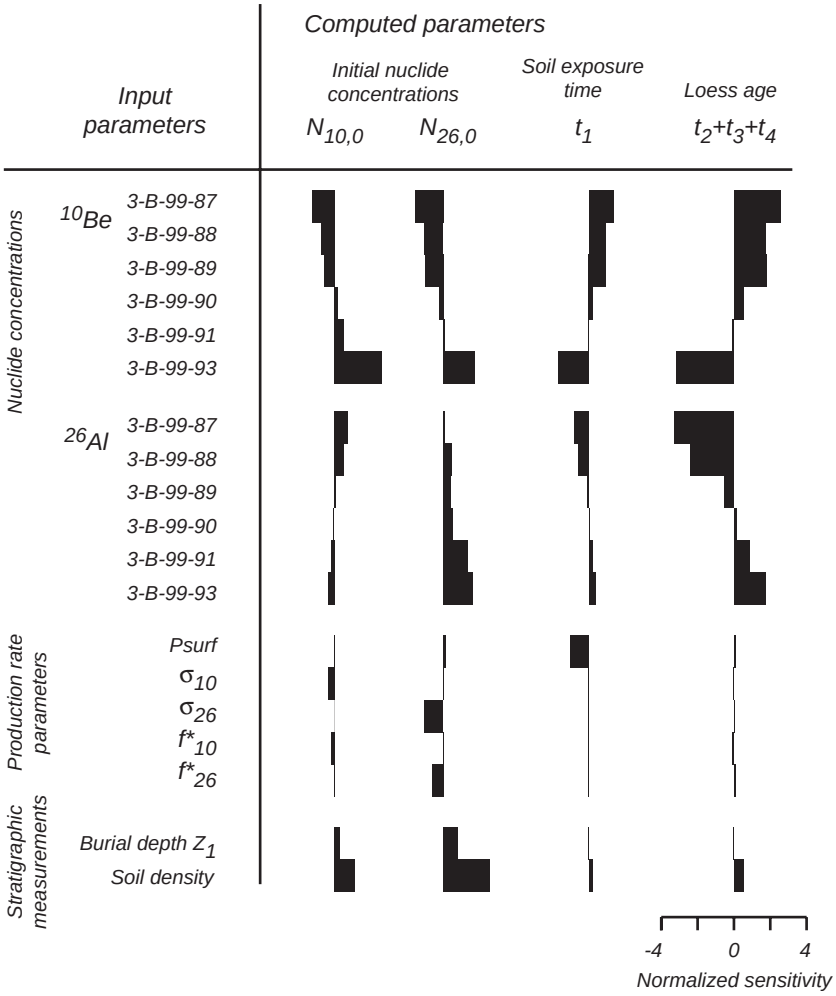

Fig. 4. Results of error analysis described in text, showing the sensitivity of the four parameters that we have estimated to the nineteen parameters that we use to evaluate the exposure model. The normalized sensitivity indicates the relative effect on an output parameter of changing the value of a particular input parameter: a normalized sensitivity of 1 indicates that a 1% increase in the input parameter results in a 1% increase in the output parameter; a value of −1 indicates a 1% decrease in the output parameter.

led us to assign incorrect values to the production rates at the sample depths during the period of soil formation. Third, the shielding depths that we used in creating the exposure model could be incorrect, either because of the uncertainty in the soil density measurements or because of inaccuracy in the assumed shielding thicknesses of the loess units, which in turn could arise because of uncertainties either in our assumptions about loess density or in the assumption that the loess thicknesses did not change since deposition. In order to evaluate the relative importance of these sources of error, we carried out an error analysis in two ways: first, by a Monte Carlo simulation, and, second, by assuming that the solution was locally linear with respect to the input parameters and numerically computing the partial derivative of each output parameter with respect to each input parameter by a first-order finite difference approximation, then adding in quadrature to compute a total uncertainty. The two approaches yielded similar results. We considered a total of nineteen input parameters: six ^{10}Be and six ^{26}Al measurements; the surface production rate of ^{10}Be (the surface production rate of ^{26}Al is linked to that of ^{10}Be by the production ratio of 6.1 and is therefore not an independent parameter itself); the muon interaction cross-sections used in computing the subsurface nuclide production rates; the soil density used in computing the sample depths during time period t_1, and the thickness of the lowermost loess unit. This last parameter accounts for both uncertainty in our assumed density and in our assumed stratigraphic thickness for this unit. We did not consider a similar uncertainty for the upper loess units because by the time they are emplaced, the sample is already relatively deeply buried, to a depth where the change in production rates with depth is very small; hence uncertainty in the thickness of these upper loesses is much less significant than for the lower loess.

Figs. 4 and 5 show the results of the error analysis. For the unknown parameters of greatest geological significance, that is, t_1 and t_2, which determine the age of the till and the lowermost loess, the analytical uncertainties in ^{26}Al and ^{10}Be measurements are by far the dominant uncertainty. Uncertainties in subsurface production rates by muons are negligible by comparison. For example, if we were to use a set of muon interaction cross-sections inferred from a quarry profile at Wyangla, Australia (J. Stone, unpublished data) that predict subsurface production rates up to 50% lower than those suggested by [27] and [28], our inferred ages for the till and the lowermost loess

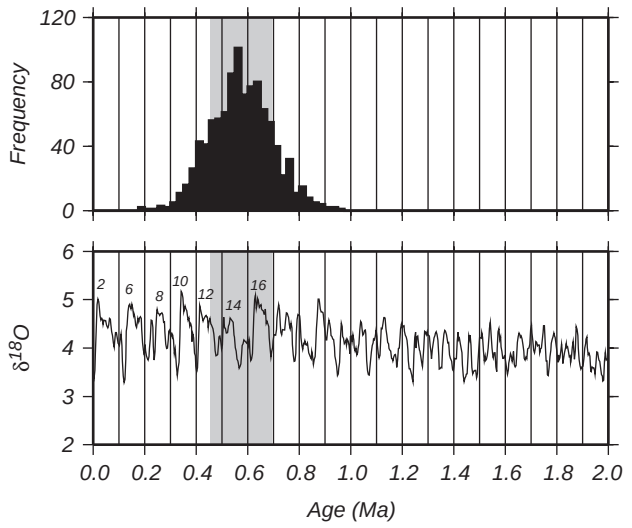

Fig. 5. Histogram of best-fit burial ages for lowest loess generated by 1000-point Monte Carlo simulation described in text, compared with the benthic oxygen-isotope record from [34]. Note that we have not included the uncertainty in the experimental determinations of the ^{10}Be and ^{26}Al decay constants, which should strictly be included when comparing ^{26}Al/^{10}Be age determinations with other time scales. In this case these uncertainties (2–3%) are small compared to the uncertainties in measuring ^{26}Al and ^{10}Be and do not significantly affect the results.

would change by less than 2%, significantly less than the analytical uncertainty. This is because the nuclide concentration developed during the period of soil formation is significantly greater than the subsequent nuclide production after the soil was buried. Thus, the subsequent change in nuclide concentrations largely reflects decay of the preexisting nuclide inventory rather than the new nuclide production at depth. In a situation where the period of soil formation was shorter and the subsequent depth of burial was less, the uncertainty in subsurface nuclide production by muons would become important.

Uncertainty in the surface nuclide production rates affects our estimate of t_1 (and therefore the age of the till), but has a minimal affect on our estimate of t_2 (and therefore the age of the loess). Uncertainty in our measured value for soil density has a minimal effect on our estimate of t_1, but a moderate effect on our estimate of t_2, although it is still less important than the analytical uncertainty.

Our estimates of the inherited nuclide concentrations in the till at the time of emplacement are less sensitive to the analytical uncertainties, but more sensitive to the other uncertainties, in particular to the uncertainties in soil density, initial burial depth, and the muon interaction cross-sections.

We derived a summary uncertainty for the ages of the loess and till, as well as the inherited nuclide concentrations in the till, using a 1000-point Monte Carlo simulation with the following random variables as input: ^{26}Al and ^{10}Be measurements assumed Gaussian with the standard errors reported in Table 2; surface production rates assumed Gaussian with the uncertainty reported in [26]; muon interaction cross-sections assumed Gaussian with mean and standard errors reported in [27] and [28]; soil density assumed Gaussian with a 5% standard error; and the shielding thickness of the lowermost loess assumed Gaussian with a 5% standard error. In evaluating the uncertainty in the age of the till we also included the surface erosion rate during soil formation as an additional random variable, assumed uniform between 3 and 8 μm yr^{-1}.

8. Conclusions

The results of the error analysis are that the loess was deposited 0.58±0.12 Ma, the till was deposited 0.65±0.14 Ma, and the initial ^{10}Be and ^{26}Al concentrations in the till were $7.8\pm0.9\times10^4$ and $2.56\pm0.6\times10^5$ atoms g^{-1}, respectively. The uncertainties in the till and loess ages, of course, are not independent; the till must always be older than the loess by at least the value of t_1. We conclude that the till was most likely emplaced during marine isotope stage 16, ca. 0.62–0.64 Ma, which is consistent with observations that the uppermost till at other sites in eastern Nebraska is normally magnetized and underlies the Lava Creek ash. The lowermost loess was most likely deposited during marine isotope stages 14 and 15, ca. 0.55–0.6 Ma.

The estimated initial ^{10}Be and ^{26}Al concentrations in quartz from the till are similar to concentrations we have observed in other Pleistocene tills, as well as modern river sediments derived therefrom, in the north-central U.S. [29]. The initial ^{26}Al/^{10}Be ratio is significantly less than the production ratio of 6.1, indicating that the samples had a complex exposure and burial history of more than 1 Ma prior to incorporation in the till. This observation underscores the need for the very general approach we have used here: the conventional assumptions used in burial dating would yield misleading ages in this situation.

The analytical uncertainties cause our final error estimate to be large: we cannot uniquely associate the age of the loess with a specific marine δ^{18}O event. However, our approach provides a means of assigning numerical ages to many Plio-Pleistocene terrestrial sediment sequences that cannot be dated by other means. It can be used wherever quartz-bearing paleosols are embedded within sedimentary sequences; and promises a significant improvement on our present ability to date and correlate Plio-Pleistocene terrestrial glacial sediments. At present, the precision of the ^{26}Al and ^{10}Be measurements is the primary limitation on the precision of the age determinations, which provides a strong incentive toward improving analytical techniques for cosmic-ray-produced nuclides, as well as incorporating other nuclides such as ^{36}Cl that would provide a more favorable set of decay constants. Other uncertainties, in particular uncertainties in subsurface production rates, are less important, and will not become a major obstacle to using this technique until ^{10}Be and ^{26}Al analyses become more precise.

Acknowledgements

Balco was supported by a graduate fellowship from the Fannie and John Hertz Foundation, by a graduate fellowship from DOSECC, and by the J. Hoover Mackin Award of the Geological Society of America. Travel and analytical work were supported by National Science Foundation grant EAR-0207844. Drilling and core collection were supported by the USGS Statemap Program. We appreciate an extremely comprehensive review by Milan Pavich, as well as an additional anonymous review.

References

[1] C. Emiliani, Pleistocene temperatures, J. Geol. 63 (1955) 538–578.
[2] N.J. Shackleton, N.D. Opdyke, Oxygen-isotope and paleomagnetic stratigraphy of equatorial Pacific core V28-238: oxygen isotope temperatures and ice volumes on a 10^5 and 10^6 year scale, Quat. Res. 3 (1973) 39–55.
[3] N.J. Shackleton, J. Backman, H. Zimmerman, D.V. Kent, M.A. Hall, D.G. Roberts, D. Schnitker, J.G. Baldauf, A. Desprairies, R. Homrighausen, P. Huddlestun, J.B. Keene, A.J. Kaltenback, K.A.O. Krumsiek, A.C. Morton, J.W. Murray, J. Westberg-Smith, Oxygen isotope calibration of the onset of ice-rafting and history of glaciation in the North Atlantic region, Nature 307 (1984) 620–623.
[4] J. Mangerud, E. Jansen, J.Y. Landvik, Late Cenozoic history of the Scandinavian and Barents Sea ice sheets, Glob. Planet. Change 12 (1996) 11–26.
[5] Michael J. Hambrey, Peter J. Barrett, Ross D. Powell, Late Oligocene and early Miocene glacimarine sedimentation in the SW Ross Sea, Antarctica: the record from offshore drilling, in: J.A. Dowdeswell, O.C. Colm (Eds.), Glacier-Influenced Sedimentation on High-Latitude Continental Margins. Geological Society of London, London, 2002.
[6] S.C. Cande, D.V. Kent, Revised calibration of the geomagnetic polarity timescale for the Late Cretaceous and Cenozoic, J. Geophys. Res. B, Solid Earth Planets 100 (4) (1995) 6093–6095.
[7] C.A. Gansecki, G.A. Mahood, M. McWilliams, New ages for the climactic eruptions at Yellowstone: single-crystal $^{40}Ar/^{39}Ar$ dating identifies contamination, Geology (Boulder) 26 (4) (1998) 343–346.
[8] J.C. Gosse, F.M. Phillips, Terrestrial in situ cosmogenic nuclides: theory and application, Quat. Sci. Rev. 20 (14) (2001) 1475–1560.
[9] J. Klein, R. Middleton, R. Giegengack, P. Sharma, Revealing histories of exposures using in situ produced ^{26}Al and ^{10}Be in Libyan desert glass, Radiocarbon 28 (1988) 547–555.
[10] D.E. Granger, P.F. Muzikar, Dating sediment burial with in situ-produced cosmogenic nuclides: theory, techniques, and limitations, Earth Planet. Sci. Lett. 188 (1–2) (2001) 269–281.
[11] T.C. Partridge, D.E. Granger, M. Caffee, R.J. Clarke, Lower Pliocene hominid remains from Sterkfontein, Science 300 (5619) (2003) 607–612.
[12] J.A. Mason, Surficial geology of the Fort Calhoun and Kennard quadrangles, Nebraska. Conservation and Survey Division Open-File Report 56, 2001.
[13] M. Roy, P.U. Clark, R.W. Barendregt, J.R. Glasmann, R.J. Enkin, Glacial stratigraphy and paleomagnetism of late Cenozoic deposits of the north-central United States, Geol. Soc. Amer. Bull. 116 (1/2) (2004) 30–41.
[14] J. Boellstorff, Chronology of some late Cenozoic deposits from the central United States and the ice ages, Trans. Nebr. Acad. Sci. VI (1978) 35–48.
[15] S.L. Forman, E.A. Bettis III, T.J. Kemmis, B.B. Miller, Chronologic evidence for multiple periods of loess deposition during the late Pleistocene in the Missouri and Mississippi River Valley, United States: implications for the activity of the Laurentide Ice Sheet, Palaeogeogr. Palaeoclimatol. Palaeoecol. 93 (1992) 71–83.
[16] S.L. Forman, J. Pierson, Late Pleistocene luminescence chronology of loess deposition in the Missouri and Mississippi River valleys, United States, Palaeogeogr. Palaeoclimatol. Palaeoecol. 186 (2002) 25–46.
[17] E.A. Bettis III, D.R. Muhs, H.M. Roberts, A.G. Wintle, Last Glacial loess in the conterminous U.S.A., Quat. Sci. Rev. 22 (2003) 1907–1946.
[18] R.G. Ditchburn, N.E. Whitehead, The separation of ^{10}Be from Silicates, Third workshop of the South Pacific Environmental Radioactivity Association, 1994, pp. 4–7.
[19] J. Stone, Extraction of Al and Be from quartz for isotopic analysis. UW Cosmogenic Nuclide Lab Methods and Procedures. Online: URL http://depts.washington.edu/cosmolab/chem.html, 2004.
[20] J.O.H. Stone, L.K. Fifield, J. Beer, M. Vonmoos, C. Obrist, M. Grajcar, P. Kubik, R. Muscheler, R. Finkel, M. Caffee, Co-precipitated silver-metal oxide aggregates for accelerator mass spectrometry of ^{10}Be and ^{26}Al, Nucl. Instrum. Methods Phys. Res., B Beam Interact. Mater. Atoms 223–224 (2004) 272–277.
[21] B.H. Sheldrick (Ed.), Analytical Methods Manual 1984. Land Resource Research Institute, Research Branch, Agriculture Canada, 1984.
[22] G. Balco, Measuring the density of rock, sand, and till. UW Cosmogenic Nuclide Lab Procedures. Online: URL http://depts.washington.edu/cosmolab/chem.html, 2004.
[23] A.R. Gillespie, P.R. Bierman, Precision of terrestrial exposure ages and erosion rates estimated from analysis of cosmogenic isotopes produced in situ, J. Geophys. Res. 100 (B12) (1995) 24637–24649.
[24] J.O.H. Stone, J.M. Evans, L.K. Fifield, G.L. Allan, R.G. Cresswell, Cosmogenic chlorine-36 production in calcite by muons, Geochim. Cosmochim. Acta 62 (3) (1998) 433–454.
[25] A. Wolkowinsky, D. Granger, Early Pleistocene incision of the San Juan River, Utah, dated with ^{26}Al and ^{10}Be, Geology 32 (2004) 749–752.

[26] J.O. Stone, Air pressure and cosmogenic isotope production, J. Geophys. Res. 105 (B10) (2000) 23753–23759.
[27] B. Heisinger, D. Lal, A.J.T. Jull, P. Kubik, S. Ivy-Ochs, K. Knie, E. Nolte, Production of selected cosmogenic radionuclides by muons: 2. Capture of negative muons, Earth Planet. Sci. Lett. 200 (3–4) (2002) 357–369.
[28] B. Heisinger, D. Lal, A.J.T. Jull, P. Kubik, S. Ivy-Ochs, S. Neumaier, K. Knie, V. Lazarev, E. Nolte, Production of selected cosmogenic radionuclides by muons: 1. Fast muons, Earth Planet. Sci. Lett. 200 (3–4) (2002) 345–355.
[29] G. Balco, The sedimentary record of subglacial erosion beneath the Laurentide Ice Sheet. Unpublished PhD thesis, University of Washington, 2004.
[30] Mathworks, Optimization Toolbox User's Guide. The Mathworks, Natick, MA, 2000.
[31] D.E. Granger, J.W. Kirchner, R.C. Finkel, Quaternary downcutting rate of the New River, Virginia, measured from differential decay of cosmogenic ^{26}Al and ^{10}Be in cave-deposited alluvium, Geology 25 (2) (1997) 107–110.
[32] D.E. Granger, D. Fabel, A.N. Palmer, Pliocene–Pleistocene incision of the Green River, Kentucky, determined from radioactive decay of cosmogenic ^{26}Al and ^{10}Be in Mammoth Cave sediments, Geol. Soc. Amer. Bull. 113 (7) (2001) 825–836.
[33] D. Lal, In situ produced cosmogenic isotopes in terrestrial rocks, Annu. Rev. Earth Planet. Sci. 16 (1988) 355–388.
[34] N.J. Shackleton, New data on the evolution of Pliocene climate variability, in: E. Vrba, G.H. Denton, T.C. Partridge, L.C. Burckle (Eds.), Paleoclimate and Evolution, with Emphasis on Human Origins, Yale, New Haven, 1995, pp. 242–248.